Grundhöfer, Lars; Gewies, Stefan; Del Galdo, Giovanni:

Estimation bounds of beat signal in the R-mode localization system

Original published in:	IEEE access / Institute of Electrical and Electronics Engineers. - New York, NY : IEEE. - 9 (2021), p. 69278-69286.
Original published:	2021-02-16
ISSN:	2169-3536
DOI:	10.1109/ACCESS.2021.3076845
[*Visited:*	2021-05-27]

IEEE Access
Multidisciplinary | Rapid Review | Open Access Journal

Received March 26, 2021, accepted April 14, 2021, date of publication April 30, 2021, date of current version May 14, 2021.

Digital Object Identifier 10.1109/ACCESS.2021.3076845

Estimation Bounds of Beat Signal in the R-Mode Localization System

LARS GRUNDHÖFER[1], (Graduate Student Member, IEEE), STEFAN GEWIES[1], AND GIOVANNI DEL GALDO[2,3], (Member, IEEE)

[1]German Aerospace Center, Institute of Communications and Navigation, 17235 Neustrelitz, Germany
[2]Institute of Information Technology, Technische Universität Ilmenau, 98693 Ilmenau, Germany
[3]Fraunhofer Institute for Integrated Circuits IIS, 91058 Erlangen, Germany

Corresponding author: Lars Grundhöfer (lars.grundhoefer@dlr.de)

This work was supported by the R-Mode Baltic Project by the European Union through the European Regional Development Fund within the Interreg Baltic Sea Region Program.

ABSTRACT The R-Mode system is a terrestrial navigation system currently under development, which exploits existing means of medium frequency radio transmission. The positioning and timing performance depends on the estimation of the signals' phase offset, from which the ranging information is derived. For an analogous problem such as the single-tone phase estimation, the Cramér-Rao bound (CRB) describes the minimal achievable performance in the mean squared error sense. For R-Mode, the problem involves the estimation of the phase offset for a beat signal, which can be described as the difference of phase estimation for the two aiding carriers next to the signal. This estimates are not statistically independent for finite observation, as we show in this paper. The effect becomes stronger for short observation times, which are important for a near real time application. In this contribution, we are interested in phase offset estimation for the signal models relevant to R-Mode: a beat signal and a beat signal combined with an MSK signal. A closed-form lower CRB is proposed for the aforementioned signal models phase estimation, as well as a generalization of the bound for the phase-difference estimation. Based on this derivation, optimized bit sequences are shown to improve performance of the estimates. The validity of the proposal is verified based on a simulation setup. Measurements acquired during a measurement campaign serve to further justify the usefulness of the bound. Some possible applications of such a bound are R-Mode coverage prediction and the associated phase estimators' performance.

INDEX TERMS CRB, phase estimation, navigation, R-Mode, signal processing.

I. INTRODUCTION

Global navigation satellite systems (GNSS) are the backbone for today's position, navigation and timing (PNT) information. Previously, several positioning and navigation systems were accessible for the maritime environment, based on different working principles, such as the LOng RAnge Navigation (LORAN), Chayka or Decca. With the increasing popularity of GNSS, the aforementioned systems were gradually shutdown in Europe. The proliferation of radio threats to GNSS signals has raised severe concerns regarding the vulnerability of the timing and navigation processes [1], [2]. The importance of such vulnerabilities is especially relevant within the maritime domain [3]–[5], making evident the need for alternative means of navigation.

One candidate is R(anging)-Mode, which exploits existing maritime signals of opportunity to procure PNT information and serves as a GNSS backup [6]. Within R-Mode, two approaches can be distinguished based on the used frequency band. The first utilizes VHF transmission, by using either the Automatic Identification System (AIS) system [7] or the upcoming standard VHF Data Exchange System (VDES) [8], [9] to provide positioning and timing. A limiting factor of VHF-based localization relates to the line-of-sight reception capabilities [10].

The second approach employs the transmission over medium frequencies (MF) of maritime differential GNSS (DGNSS) services. Such a DGNSS service transmits relevant GNSS correction data from stations situated on shore sides. The information is modulated as Minimum Shift Keyed (MSK) in the band from 283.5 kHz to 325 kHz with a region-dependent bandwidth of 500 Hz or 1 kHz and data

The associate editor coordinating the review of this manuscript and approving it for publication was Prakasam Periasamy.

rates of 50 to 200 bits/s [11]. In Europe, the channel bandwidth is 500 Hz and the most commonly used data rate is 100 bits/s [12]. As MF signals propagate as ground waves, their use is not restricted to the line-of-sight, and the existing infrastructure covers most high-density traffic areas of up to 500 km from the shore [13]. Thus, R-Mode based on MF transmission constitutes the focus of our work.

To obtain precise ranging, two single tones (CW) are introduced, symmetrical around the carrier frequency, in the zero crossings of the MSK spectra of the DGNSS transmitted signal [14]. The added tones are transmitted such that their zero crossings appear at full seconds at the transmitter antenna. Fig. 1 depicts an example of the spectrum for the resulting signal, with an MSK-modulated signal at $f_c = 303.5$ KHz and single tones at $f_c \pm 225$ Hz. Analogously to GNSS carrier-phase observations, the direct phase estimation for the aforementioned two tones would lead to a precise and ambiguous pseudorange measurement, with ambiguities of ~ 1 km. Alternatively, one can derive a beat signal from the two tones by taking the phase difference over time, avoiding dealing with ambiguity resolution. The resulting signal has a frequency of 450 Hz and the phase offset at the full second is derived by a simple subtraction of the estimates of both single tones.

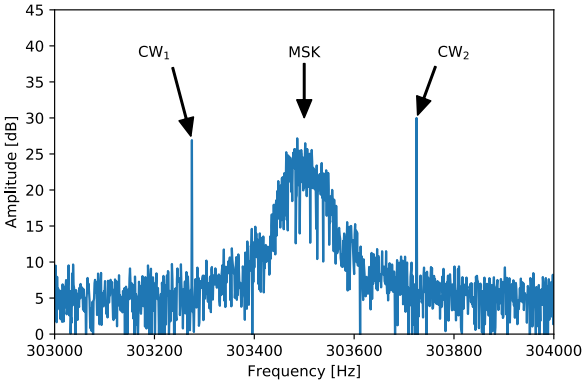

FIGURE 1. Spectra of the simulated measurements from the station Zeven (Germany) for a sample rate of 1 MS/s. CW_1 and CW_2 point to the upper and lower tone, with the MSK pointing to the signal due to modulation.

When addressing a new estimation problem, in this case localization based on MF beat signals, it is of fundamental relevance to characterize the ultimate achievable performance of the problem. The derivation of tight-performance lower bounds responds to these needs. Lower bounds can be categorized in *Bayesian* and *deterministic*. The first consider the unknown parameters as random variables with an *a priori* probability and evaluate the globally best estimator, while the latter consider the unknown parameters as deterministic and evaluate the locally best estimator performance [15]. In this work, we are interested in deriving a *deterministic* Cramér-Rao bound (CRB) for the amplitude and phase of a beat signal.

This information is a precondition for the estimation if resolving the ambiguities of the single-tones in a certain region is possible and improves the choice of estimation parameter in the receiver. A related lower bound is derived for the estimation of a single-tone phase [16]. The bound is used for coverage prediction and as an overall measure of system performance. Currently, the beat frequency is not covered by this bound and is subject to ongoing research [17].

In this work, we show that the estimates of the tones for the described R-Mode signal are not statistically independent for finite observation, so they cannot be considered as separate sinusoids as in [18]. Based on our derivation of the bound, we show optimized bit patterns that nearly satisfy statistical independence of R-Mode signal components, which is a prerequisite for an optimized navigation message, that minimizes the variance of CW phase estimation.

The article is organized as follows: Section 2 introduces the basics on Cramér-Rao lower bounds. Section 3 details the three signal models of interest and their associated CRBs. Section 4 and 5 present the results and discussion based on simulated and real scenarios, respectively. Finally, Section 6 presents the conclusion and future work.

II. CRAMÉR-RAO LOWER BOUND

The CRB is the most well-known lower bound due to its easiness of derivation and being the lowest bound on the variance of any unbiased estimator [19]. This section provides an overview of the CRB computation for a generic discrete-time signal model, given as

$$s(t_n, \boldsymbol{\theta}) \text{ with } \boldsymbol{\theta} = [\Theta_1, \Theta_2, \dots \Theta_a]^\top, \quad n = 0, \dots, N-1. \tag{1}$$

Here $\boldsymbol{\theta}$ is the unknown parameter vector with a components Θ_i, t_n denotes discrete time and n is the index of the time step currently evaluated.

We represent the samples we want use for estimation in the sampled vector $\boldsymbol{x}$ with length N. The nth element $X[n]$ of vector $\boldsymbol{x}$ is defined as

$$X[n] = s(t_n, \hat{\boldsymbol{\theta}}) + w[n], \tag{2}$$

with $\hat{\boldsymbol{\theta}}$ the true value of the parameters. Moreover, the noise is described by the zero-mean Gaussian noise vector $\boldsymbol{w}$ with variance σ^2 and his nth element $w[n]$. Under this assumption, we obtain the likelihood function for the signal model according to [19].

For a multi-parameter model, the Cramér-Rao lower bound is given by

$$\text{var}(\Theta_i) \geq \boldsymbol{J}^{-1}(\boldsymbol{\theta})_{ii}, \tag{3}$$

with $\boldsymbol{J}^{-1}(\boldsymbol{\theta})_{ii}$ the ith diagonal element of the inverse Fisher Information Matrix (FIM) $\boldsymbol{J}^{-1}(\boldsymbol{\theta})$ [18]. The coefficient of the FIM $\boldsymbol{J}(\boldsymbol{\theta})$ can be calculated as

$$\boldsymbol{J}(\boldsymbol{\theta})_{ij} = \frac{1}{\sigma^2} \sum_{n=0}^{N-1} \frac{\partial\, s(t_n, \boldsymbol{\theta})}{\partial \Theta_i} \frac{\partial\, s(t_n, \boldsymbol{\theta})}{\partial \Theta_j}, \tag{4}$$

which is the real part of the calculation in [16]. The representation in (4) simplified the derivation for the bound [19] and is used in the following sections.

III. LOWER BOUND FOR PHASE DIFFERENCE

A. ADDITIVE SIGNAL MODEL

The first signal model considered relates to the estimation of phase difference of two tones, which describe the beat signal, within noise for an additive signal model

$$s_{\text{add}}(t_n, \boldsymbol{\varphi}) = A_1 \sin(\omega_1 t_n + \varphi_1) + A_2 \sin(\omega_2 t_n + \varphi_1 + \varphi_{\text{beat}}). \quad (5)$$

We add two sinusoids with only the circular frequencies ω_1 and ω_2 known. While the first sinus term presents a phase offset φ_1, the second term comprises the phase difference $\varphi_{\text{beat}} + \varphi_1$. Each tone displays independent amplitudes A_1 and A_2. Thus, the unknowns lead to the parameter vector

$$s_{\text{add}}(t_n, \boldsymbol{\varphi}) \text{ with } \boldsymbol{\varphi} = [\varphi_1, A_1, A_2, \varphi_{\text{beat}}]^\top. \quad (6)$$

We can obtain the first derivatives of each parameter as

$$\frac{\partial s_{\text{add}}(t_n, \boldsymbol{\varphi})}{\partial \varphi_1} = A_1 \cos(\omega_1 t_n + \varphi_1) + A_2 \cos(\omega_2 t_n + \varphi_1 + \varphi_{\text{beat}}), \quad (7)$$

$$\frac{\partial s_{\text{add}}(t_n, \boldsymbol{\varphi})}{\partial \varphi_{\text{beat}}} = A_2 \cos(\omega_2 t_n + \varphi_1 + \varphi_{\text{beat}}), \quad (8)$$

$$\frac{\partial s_{\text{add}}(t_n, \boldsymbol{\varphi})}{\partial A_1} = \sin(\omega_1 t_n + \varphi_1), \quad (9)$$

$$\frac{\partial s_{\text{add}}(t_n, \boldsymbol{\varphi})}{\partial A_2} = \sin(\omega_2 t_n + \varphi_1 + \varphi_{\text{beat}}). \quad (10)$$

Let us assume that the observations contain an integer number of seconds and that our frequencies are multiples of 1 Hz. The following therefore applies for any angle ϕ

$$\frac{1}{N} \sum_{n=0}^{N-1} \cos(\omega_k t_n + \phi) = 0. \quad (11)$$

Thus, the resulting FIM is as follows

$$\boldsymbol{J}_{\text{add}}(\boldsymbol{\varphi}) = \frac{N}{2\sigma^2} \begin{pmatrix} A_1^2 + A_2^2 & 0 & 0 & A_2^2 \\ 0 & 1 & 0 & 0 \\ 0 & 0 & 1 & 0 \\ A_2^2 & 0 & 0 & A_2^2 \end{pmatrix}, \quad (12)$$

whose inverse is the CRB for (5) under assumption (11)

$$\boldsymbol{J}_{\text{add}}^{-1}(\boldsymbol{\varphi}) = \frac{2\sigma^2}{N} \begin{pmatrix} \frac{1}{A_1^2} & 0 & 0 & -\frac{1}{A_1^2} \\ 0 & 1 & 0 & 0 \\ 0 & 0 & 1 & 0 \\ -\frac{1}{A_1^2} & 0 & 0 & \frac{1}{A_1^2} + \frac{1}{A_2^2} \end{pmatrix}. \quad (13)$$

Applying (3), the minimum variance of the estimate of the unknown phase parameters is obtained

$$\text{var}(\varphi_1) \geq \frac{2\sigma^2}{N A_1^2}, \quad (14)$$

$$\text{var}(\varphi_{\text{beat}}) \geq \frac{2\sigma^2}{N} \left(\frac{1}{A_1^2} + \frac{1}{A_2^2} \right), \quad (15)$$

The derived result for φ_1 corresponds to the bound in literature for a single tone, beside a factor of two [16]. This factor occurs as we evaluate real valued signal, where in literature a complex model was chosen. Moreover, the bound for the phase difference equals the sum of the variance, given that each frequency is estimated independently. Therefore, in the asymptotic regimen case for which the lower bound is attained by an estimator, the estimation of each signal part is statistically independent.

B. ADDITIVE SIGNAL MODEL WITH MSK SIGNAL

In our problem of interest, the additive signal previously described is found in combination with an MSK signal that encodes the DGNSS correction data. In a time-discrete domain, an MSK modulated bit sequence b_k can be written as

$$s_{\text{MSK}}(t_n) = \sin(\omega_c t_n + b_k[n] \frac{\pi t_n}{2T} + \bar{\varphi}_k), \quad (16)$$

where ω_c is the circular frequency of the modulated signal, T is the bit duration, $b_k[n]$ is the bit sequence and $\bar{\varphi}_k$ is the memory of the MSK [20]. We interpret $b_k[n]$ as a sampled vector, that repeats minus ones or ones for a bit duration T. This leads to an overall vector length of N. The vector $\bar{\varphi}_k$, is handled in a similar way, as we satisfy again that the vector has the length N. Furthermore, we assume that ω_c and T are known in advance.

We include the discrete modulated MSK signal in our existing signal model (5), which leads to

$$s_{\text{signal}}(t_n, \boldsymbol{\varphi}) = A_1 \sin(\omega_1 t_n + \varphi_1) + A_c \sin(\omega_c t_n + b_k[n] \frac{\pi t_n}{2T} + \varphi_1 + \varphi_k) + A_2 \sin(\omega_2 t_n + \varphi_1 + \varphi_{\text{beat}}), \quad (17)$$

where A_c is the amplitude of the modulated signal part. Moreover, the phase difference between signals with frequency ω_1 and ω_c can be described as part of φ_k. In this case, the vector of parameters is extended to

$$s_{\text{signal}}(t_n, \boldsymbol{\varphi}) \text{ with } \boldsymbol{\varphi} = [\varphi_1, \varphi_k, \varphi_{\text{beat}}, b_k[n], A_1, A_c, A_2]^\top. \quad (18)$$

In order to derive the bound accordingly, the partial derivatives are as follows

$$\frac{\partial s_{\text{signal}}(t_n, \boldsymbol{\varphi})}{\partial \varphi_1} = A_1 \cos(\omega_1 t_n + \varphi_1) + A_c \cos(\omega_k t_n + b_k[n] \frac{\pi t_n}{2T} + \varphi_1 + \varphi_k) + A_2 \cos(\omega_2 t_n + \varphi_1 + \varphi_{\text{beat}}), \quad (19)$$

$$\frac{\partial s_{\text{signal}}(t_n,\boldsymbol{\varphi})}{\partial \varphi_k} = A_c \cos(\omega_k\, t_n + b_k[n]\frac{\pi\, t_n}{2\, T} + \varphi_1 + \varphi_k), \tag{20}$$

$$\frac{\partial s_{\text{signal}}(t_n,\boldsymbol{\varphi})}{\partial \varphi_{\text{beat}}} = A_2 \cos(\omega_2\, t_n + \varphi_1 + \varphi_{\text{beat}}), \tag{21}$$

$$\frac{\partial s_{\text{signal}}(t_n,\boldsymbol{\varphi})}{\partial b_k[n]} = A_c \frac{\pi\, t_n}{2\, T} \cos(\omega_k\, t_n + b_k[n]\frac{\pi\, t_n}{2\, T} + \varphi_1 + \varphi_k), \tag{22}$$

$$\frac{\partial s_{\text{signal}}(t_n,\boldsymbol{\varphi})}{\partial A_1} = \sin(\omega_1\, t_n + \varphi_1), \tag{23}$$

$$\frac{\partial s_{\text{signal}(t_n,\boldsymbol{\varphi})}}{\partial A_c} = \sin(\omega_c\, t_n + b_k[n]\frac{\pi\, t_n}{2\, T} + \varphi_1 + \varphi_k), \tag{24}$$

$$\frac{\partial s_{\text{signal}}(t_n,\boldsymbol{\varphi})}{\partial A_2} = \sin(\omega_2\, t_n + \varphi_1 + \varphi_{\text{beat}}). \tag{25}$$

For calculating the FIM for this signal model, let us resort to assumption (11) again and extend it for the modulated signal, such that

$$S_{\text{sum}} = \frac{1}{N}\sum_{n=0}^{N-1} \cos(\omega\, t_n + b_k[n]\frac{\pi\, t_n}{2\, T} + \varphi_1 + \varphi_k) \approx 0. \tag{26}$$

Assumption (26) shall hold valid for certain bit patterns, provided that the memory of the MSK is zero at each second, and we sum up an integer number of wavelengths of ω_c. Moreover, we need to assume

$$S_{\text{linear}} = \frac{1}{N}\sum_{n=0}^{N-1} \left(\frac{\pi\, t_n}{4\, T}\right) \times \cos(\omega\, t_n + b_k[n]\frac{\pi\, t_n}{2\, T} + \varphi_k - \varphi_{beat}) \approx 0, \tag{27}$$

and

$$S_{\text{squared}} = \frac{1}{N}\sum_{n=0}^{N-1} \left(\frac{\pi\, t_n}{2\, T}\right)^2 \times \cos(\omega\, t_n + b_k[n]\frac{\pi\, t_n}{2\, T} + \varphi_1 + \varphi_k) \approx 0, \tag{28}$$

with ω any integer frequency, to obtain a closed form for the CRB.

In order to solve the sum over the derivations, we need to substitute $t_n = \frac{n}{f_{\text{sample}}}$ and $T = \frac{N_{\text{bit}}}{f_{\text{sample}}}$. Here, f_{sample} is the sample rate of the observation and N_{bit} is the bit duration in number of samples.

The resulting FIM calculated under the previous assumptions leads to

$$\boldsymbol{J}_{\text{signal}}(\boldsymbol{\varphi}) = \frac{N}{2\,\sigma^2}\begin{pmatrix} \boldsymbol{J}_{4\times4} & \boldsymbol{0}_{4\times3} \\ \boldsymbol{0}_{4\times3}^{\top} & \boldsymbol{I}_{3\times3} \end{pmatrix}, \tag{29}$$

with $\boldsymbol{I}_{3\times3}$ the unit matrix of size 3 and $0_{4\times3}$ the null matrix of size 4×3. The $J_{4\times4}$ is given by (31), as shown at the bottom of the page. The inverse of the FIM in the MSK case can be found as

$$J^{-1}_{\text{signal}}(\boldsymbol{\varphi}) = \frac{2\,\sigma^2}{N}\begin{pmatrix} \boldsymbol{J}^{-1}_{4\times4} & \boldsymbol{0}_{4\times3} \\ \boldsymbol{0}_{3\times4} & \boldsymbol{I}_{3\times3} \end{pmatrix}, \tag{30}$$

with $\boldsymbol{J}^{-1}_{4\times4}$ defined in (32), as shown at the bottom of the page. We evaluate the diagonal elements of $\boldsymbol{J}^{-1}_{\text{signal}}$ for the phase bounds and obtain

$$\text{var}(\varphi_1) \geq \frac{2\sigma^2}{N\, A_1^2}, \tag{33}$$

$$\text{var}(\varphi_k) \geq \frac{2\,\sigma^2(4\,A_1^2\,N + A_c^2\,N - 2\,A_1^2 + A_c^2)}{N\,(A_1^2\,A_c^2\,N + A_1^2\,A_c^2)}, \tag{34}$$

$$\boldsymbol{J}_{4\times4} = \begin{pmatrix} A_1^2 + A_c^2 + A_2^2 & A_c^2 & A_2^2 & \frac{\pi\, A_c^2(N-1)}{4\, N_{\text{bit}}} \\ A_c^2 & A_c^2 & 0 & \frac{\pi\, A_c^2(N-1)}{4\, N_{\text{bit}}} \\ A_2^2 & 0 & A_2^2 & 0 \\ \frac{\pi\, A_c^2(N-1)}{4\, N_{\text{bit}}} & \frac{\pi\, A_c^2\,(N-1)}{4\, N_{\text{bit}}} & 0 & \frac{\pi^2\, A_c^2\,\,(N-1)(2\,N-1)}{24\, N_{\text{bit}}^2} \end{pmatrix} \tag{31}$$

$$\boldsymbol{J}^{-1}_{4\times4} = \begin{pmatrix} \frac{1}{A_1^2} & -\frac{1}{A_1^2} & -\frac{1}{A_1^2} & 0 \\ -\frac{1}{A_1^2} & \frac{4\,A_1^2\,\text{N} + A_c^2\,\text{N} - 2\,A_1^2 + A_c^2}{A_1^2\,A_c^2\,\text{N} + A_1^2\,A_c^2} & \frac{1}{A_1^2} & -\frac{12\,N_{\text{bit}}^2}{\pi\, A_c^2\, N + \pi\, A_c^2} \\ -\frac{1}{A_1^2} & \frac{1}{A_1^2} & \frac{A_1^2 + A_2^2}{A_1^2\, A_2^2} & 0 \\ 0 & -\frac{12\, N_{\text{bit}}^2}{\pi\, A_c^2\, N + \pi\, A_c^2} & 0 & \frac{48\, N_{\text{bit}}^2}{\pi^2\, A_c^2\, N^2 - \pi^2\, A_c^2} \end{pmatrix} \tag{32}$$

$$\mathrm{var}(\varphi_{\mathrm{beat}}) \geq \frac{2\sigma^2}{N}\left(\frac{1}{A_1^2}+\frac{1}{A_2^2}\right), \tag{35}$$

The variances of the phases φ_1 and φ_{beat} are the same as for the additive model. This is also justified as in (31) there is no correlation between the modulation and the single tones [21]. It can be concluded that assuming equations (26), (27) and (28), the variance of the phase estimates remains equal, regardless of whether the bit sequence b_k is known.

Nonetheless, it has been shown that the sinusoidal signal and the MSK modulation interfere with each other, and that the influence can be mitigated if the bit sequence is known *a priori* [21]. The problem is that the assumption in (26), (27) and (28) is only an approximation, valid only if the bits are evenly distributed. Otherwise, we would be adding over an uncompleted wave, resulting in a large deviation from the assumption. In reality, the data streams do not follow such restrictions. In that case, the element J_{34} in (31) is calculated according to (4) by

$$J_{34} = \frac{1}{\sigma^2}\sum_{n=0}^{N-1}\left[\frac{A_2 A_c \pi t_n}{4T}\cos\left(b_k[n]\frac{\pi t_n}{2T}+2\varphi_1+\varphi_{\mathrm{beat}}+\varphi_k + \omega_2 t_n+\omega_c t_n\right)+\frac{A_2 A_c \pi t_n}{4T}\cos\left(b_k[n]\frac{\pi t_n}{2T}-\varphi_{\mathrm{beat}} + \varphi_k-\omega_2 t_n+\omega_c t_n\right)\right] \tag{36}$$

for non-equally distributed bits. The error introduced in relation to assumption (27) depends on the bit pattern observed. Moreover, (28) has no influence on the interference terms, as it only appears in J_{44}. Taken into consideration, the resulting bound would be invalid for the estimation of the bit pattern.

To find an optimized bit pattern, one may resort to (26) and (27). By assuming an uneven amount of 1 and -1 for the MSK bits, a phase shift is observed. In that case, the sum is not performed over an integer wave number, and the associated phase error could be large. However, when an equal number of 1s and -1s are regarded, the phase estimate would result unbiased. For this case, another source of error becomes recognizable, since a bit change leads to a mismatch in the sum at the change of the bit, and yields a small error. Such considerations will be evaluated during Section IV, where different alternating bit patterns are studied to minimize estimation errors.

To motivate (26) and (27), we evaluate the expressions for the case of the transmitter station in Zeven. Therefore, we use a bit pattern with four equal bits that are repeated with alternating signs. We obtain the values $S_{\mathrm{sum}} = -7.90\cdot 10^{-16}$ and $S_{\mathrm{linear}} = 7.85\cdot 10^{-5}$, for a frequency of $\omega = 2\pi\ 225$ Hz, a bit rate of $T = 100$bit/s and $N = 10^6$ samples. So even with a linear growing factor, the sum stays small compared to the other values in matrix (31).

One may conclude that, for calculating the lower bound with an unknown bit sequence, assumptions (26) and (27) can be considered as holding true. Although the obtained bounds for the phase estimation prove to be valid, no estimator would ever reach this bound in reality if the bit pattern estimation is disregarded.

C. PHASE DIFFERENCE IN A DYNAMIC SCENARIO

So far, only the lower bound for the case where the phase offset remains constant has been considered, which is legitimate for static transmitter and receiver ends during the sampling time. Hereinafter, the additive model is extended for a dynamic case, with a constant unknown radial velocity v, normalized to the speed of light c. Thus, the time-dependent phase offset is defined as

$$\varphi_{\mathrm{velocity}} = \omega_i\, t_n\, \frac{v}{c}. \tag{37}$$

The resulting signal model is as follows

$$s_{\mathrm{dynamic}}(n,\boldsymbol{\varphi}) = A_1\sin(\omega_1 t_n+\omega_1 t_n\frac{v}{c}+\varphi_1). + A_2\sin(\omega_2 t_n+\omega_2 t_n\frac{v}{c}+\varphi_1+\varphi_{\mathrm{beat}}) \tag{38}$$

It is now important to notice that the phase offsets φ_1 and φ_{beat} describe the phase offset at start of the observation. The phase offset change is described with the terms $\omega_1 t_n \frac{v}{c}$ and $\omega_2 t_n \frac{v}{c}$. The resulting parameter vector is

$$\boldsymbol{\varphi} = [\varphi_1, \varphi_{\mathrm{beat}}, v, A_1, A_2,]^\top. \tag{39}$$

The partial derivatives result

$$\frac{\partial s_{\mathrm{dynamic}}(t_n,\boldsymbol{\varphi})}{\partial\varphi_1} = A_1\cos\left(t_n\omega_1(\frac{v}{c}+1)+\varphi_1\right) + A_2\cos\left(t_n\omega_2(\frac{v}{c}+1)+\varphi_1+\varphi_{\mathrm{beat}}\right), \tag{40}$$

$$\frac{\partial s_{\mathrm{dynamic}}(t_n,\boldsymbol{\varphi})}{\partial\varphi_{\mathrm{beat}}} = A_2\cos\left(t_n(\omega_1\frac{v}{c}+\omega_2\frac{v}{c}+\omega_2) + \varphi_1+\varphi_{\mathrm{beat}}\right), \tag{41}$$

$$\frac{\partial s_{\mathrm{dynamic}}(t_n,\boldsymbol{\varphi})}{\partial v} = A_1\frac{\omega_1 t_n}{c}\cos\left(t_n\omega_1(\frac{v}{c}+1)+\varphi_1\right) + A_2\frac{\omega_2 t_n}{c} \times\cos\left(t_n\omega_2(\frac{v}{c}+1)+\varphi_1+\varphi_{\mathrm{beat}}\right), \tag{42}$$

$$\frac{\partial s_{\mathrm{dynamic}}(t_n,\boldsymbol{\varphi})}{\partial A_1} = \sin\left(t_n\omega_1(\frac{v}{c}+1)+\varphi_1\right), \tag{43}$$

$$\frac{\partial s_{\mathrm{dynamic}}(t_n,\boldsymbol{\varphi})}{\partial A_2} = \sin\left(t_n\omega_2(\frac{v}{c}+1)+\varphi_1+\varphi_{\mathrm{beat}}\right). \tag{44}$$

Again, we are interested in the sum over the tones with angular frequency ω, by interpreting $\frac{\omega v}{c}$ as a Doppler frequency. For an integer number of $\frac{\omega v}{c}$ we can assume

$$\sum_{\mathrm{n}=0}^{\mathrm{N}-1} n\cos(t_n\omega+(\frac{v}{c}+1)+\varphi)\approx 0. \tag{45}$$

As the shifted frequency is an integer frequency, (45) can be addressed as in (27). In a practical scenario, this assumption can only be hold true considering an unrealistic velocity,

where the observation time is defined in such a way that the sum is obtained over complete wavelengths. Under such an assumption, the FIM can be calculated as

$$\boldsymbol{J}_{\text{dynamic}}(\boldsymbol{\varphi}) = \frac{N}{2\,\sigma^2}\begin{pmatrix} \boldsymbol{J}_{3\times3} & \boldsymbol{0}_{3\times2} \\ \boldsymbol{0}_{2\times3} & \boldsymbol{I}_{2\times2} \end{pmatrix}. \tag{46}$$

As the lower bounds are now dependent on N, ω_1 and ω_2 the inverse FIM is quite complicated and beyond the scope of this paper. However, if we consider v as known, we can erase the third row and the third column of the FIM (46). As a result, we obtain an FIM that equals (13) and receive the same resulting bounds as in (15).

D. GENERALIZED BOUND

We have shown that the signal models (17) and (38) lead to the same bound for the phase as the simple additive approach (5), under the assumptions of equal bit distribution or known velocity.

Some interesting modifications for the bound would express the number of samples $N = T_{obs} f_{\text{sample}}$ with T_{obs} the observation time and f_{sample} the sampling rate. Furthermore, using the definition of signal-to-noise ratio $\text{SNR} = A^2/\sigma^2$, the general CRB form for the phase estimation for a beat signal is given by

$$\text{var}(\varphi_1) \geq \frac{2}{T_{obs} f_{\text{sample}}\,\text{SNR}_{\text{A1}}}, \tag{48}$$

$$\text{var}(\varphi_{\text{beat}}) \geq \frac{2}{T_{obs} f_{\text{sample}}}\left(\frac{1}{\text{SNR}_{\text{A1}}} + \frac{1}{\text{SNR}_{\text{A2}}}\right). \tag{49}$$

It is well known that the variance of an estimation scales with $\frac{1}{T_{obs}\,b}$, where b is the bandwidth evaluated. We see the same relation in (48), when we interpret f_{sample} as bandwidth with respect to the Nyquist–Shannon theorem. Therefore, we only reach this bound with our estimator when we evaluate the whole bandwidth and not only a portion of it. Moreover, with a variation of the sample rate, the total energy of the discrete sample signal changes and so does the signal-to-noise ratio consequently.

IV. SIMULATION

To verify the theoretical results presented above, we set up a simulation of the signal within our Python development environment. We want to show when the estimations of the single tones become statistically independent, for which

$$var(\varphi_1) + var(\varphi_2) = var(\varphi_{\text{beat}}) \tag{50}$$

must be satisfied. Here, φ_2 is the phase estimate of the second single tone.

We generate signals according to our signal models (5) and (17). The frequencies are chosen to $\omega_c = 2\pi f_c$, $f_c = 303500\,\text{Hz}$; and $\omega_1, \omega_2 = 2\pi(f_c \pm 225\,\text{Hz})$ which are the realistic frequencies of the DGNSS transmitter in Zeven. The simulated amplitudes are $A_1 = 0.001$, $A_2 = 0.002$ and $A_c = 0.004$. The bit sequence b_k, and sample rate are varied to show their influence. Moreover, we use additive white Gaussian noise for the noise floor, white the same variance σ^2 for both sample rates. Each simulation consists of a 3000 s long data set, which estimates the phase offsets φ_1 of the lower frequency tone and φ_2 of the higher frequency tone with a fast Fourier transform for an observation time of 1 s. This corresponds to a maximum likelihood estimation [22]. Here, the bandwidth of the estimator is independent of the sample rate. The phase offset of the beat frequency is obtained as the difference between the phase φ_1 and φ_2.

A. ADDITIVE SIGNAL MODEL

The simulations with the additive model were conducted with 1 MS/s and 5 MS/s. We expected that the variance of the noise would scale with the factor of 5, but we simulate a constant σ^2. Therefore, only the amplitude scales and the variance change by a factor of 1/5.

Moreover, the variance of the phase difference should be the addition of the variance of the two sinusoids as shown in Section 3. In Table 1, the results of the simulation are presented. The first columns indicate the used sample rate and the following two give the variance of the estimation of φ_1 and φ_2, respectively. The column φ_{beat} expresses the case that we calculate the phase difference and subsequently calculate the variance. The last column is the addition of the second and third column.

TABLE 1. Variance in rad^2 of the simulation results for the additive signal model.

Sample rate	φ_1	φ_2	φ_{beat}	$\varphi_1 + \varphi_2$
1 MS/s	$4.61 \cdot 10^{-6}$	$1.13 \cdot 10^{-6}$	$6.01 \cdot 10^{-6}$	$5.74 \cdot 10^{-6}$
5 MS/s	$0.89 \cdot 10^{-6}$	$0.22 \cdot 10^{-6}$	$1.11 \cdot 10^{-6}$	$1.11 \cdot 10^{-6}$

All values scale with factor 5 as expected, and we see just a minor difference between the last two columns, as predicted by the bound for this model. In this simulation, the estimations are therefore statistically independent.

$$\boldsymbol{J}_{3\times3} = \begin{bmatrix} A_1^2 + A_2^2 & A_2^2 & \frac{(N-1)\left(A_1^2\,\omega_1 + A_2^2\,\omega_2\right)}{2} \\ A_2^2 & A_2^2 & \frac{A_2^2\,\omega_2\,(N-1)}{2} \\ \frac{(N-1)\left(A_1^2\,\omega_1 + A_2^2\,\omega_2\right)}{2} & \frac{A_2^2\,\omega_2\,(N-1)}{2} & \frac{(N-1)\,(2\,N-1)\left(A_1^2\,\omega_1 + A_2^2\,\omega_2\right)}{6} \end{bmatrix} \tag{47}$$

B. ADDITIVE SIGNAL MODEL WITH MSK SIGNAL

For the signal model (17) including the modulation, we simulate a signal with 1 MS/s and 5 MS/s sample rate at a bit rate of 100 bit/s. Four different bit sequences were used: b_1 repeats the sequences $[-1,1]$, b_2 alternates $[-1,-1,1,1]$ and b_3 alternates the sequence $[-1,-1,-1,-1,1,1,1,1]$. For b_1 to b_3, the resulting sequences contain an even number of 1s and -1s. Thus, the energy introduced by the MSK modulation is reduced in the evaluated bandwidth. The sequence b_4 is generated based on a uniformly distributed random sequence, with an uneven number of -1, 1 bits. The energy introduced by the modulation needs to be considered. However, the variance should scale with $\sqrt{5}$ as the noise energy is distributed over a larger frequency space.

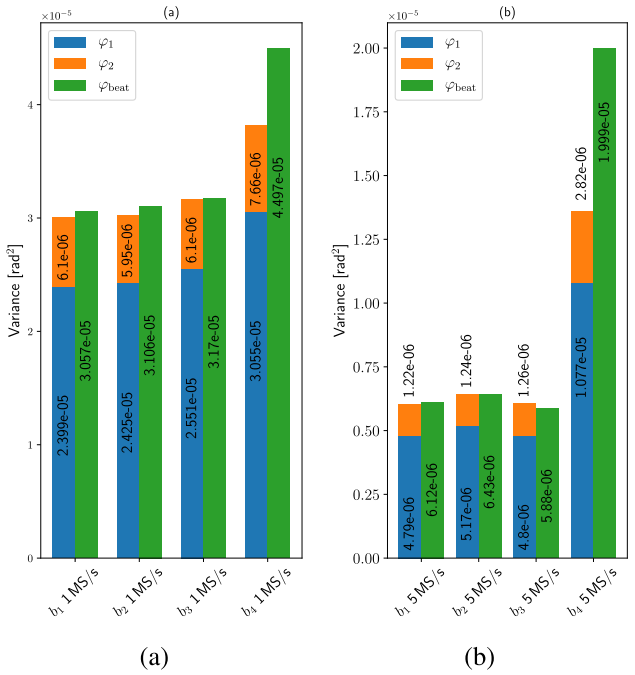

FIGURE 2. Bar plot of simulation results for the signal model with MSK for 1 MS/s (a) and 5 MS/s (b). The optimized bit sequence b_1, b_2 and b_3, show that the estimates of the continuous wave are statistically independent. This is not the case for the random bit sequence b_4.

Fig. 2(a) shows the variance in rad^2 of the different bit sequences b for 1 MS/s sample rate as bar plot. The blue bar represents the variance for φ_1 at frequency ω_1; on top of this, the orange bar marks the variance for φ_2 at frequency ω_2. By doing so, the sum of the results is comparable to the green bar, which shows the result of the variance when we calculate the beat frequency out of the estimates. Inside of each bar, the numerical value is shown. Fig. 2 (b) shows the results for 5 MS/s sampling rate in the same way as in Fig. 2 (a). Here, the numeric value for φ_2 is set on top of the bar.

We can see that the variance obtained with bit sequences b_1, b_2 and b_3 scales with the sample rate as expected with factor 5. Moreover, the variance of the Beat frequencies equals roughly the sum of the variance for the estimated two different tones as for the additive model. The differences in the resulting mismatch at the sum over the MSK signal has no significant influence. For the random distribution, where we have to consider the MSK energy, the variance scales with $\sqrt{5}$, as expected by summing up the power density function of the MSK. Moreover, the estimates of the sinusoids are no longer statistically independent, as we see the sum of the variance now differs from the variance of the beat frequencies' offset. Furthermore, the resulting variance is significantly higher than for the bit sequences with an equal bit number.

V. MEASUREMENTS

A measurement of the entire R-Mode signal with two sinusoids and an MSK signal component was conducted with the software defined radio (SDR) based R-Mode receiver platform shown in Fig. 3, which is a development of the german aerospace center (DLR) [21].

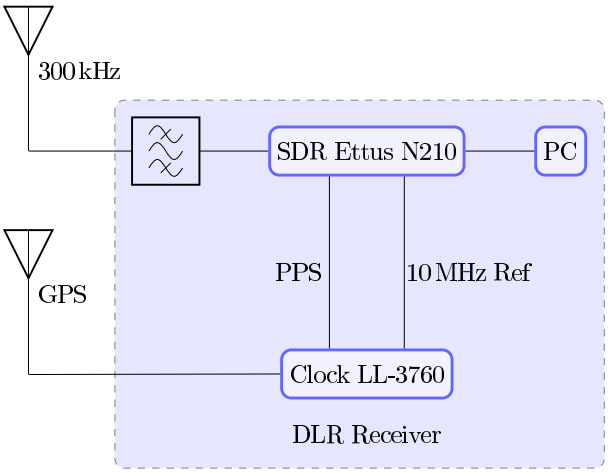

FIGURE 3. Block diagram of the DLR receiver design.

A. RECEIVER DESCRIPTION

The analog front-end uses the bandpass filter between 285 kHz and 325 kHz as antialiasing filter and to suppress noise. The filter consists of two 8-pole Bessel filters installed together with a power supply in a housing.

The SDR following the filter combines parts of the analog front end with the digital front end. In our case, we use the Ettus N210 SDR, which allows us to change the analog front-end part through the use of a daughterboard, thereby covering a huge band of use cases and a wide frequency range. In the digital part after sampling, the SDR performs some beneficial filtering. The so processed data are sent to a personal computer via Ethernet.

Considering the low number of R-Mode transmitters and for the sake of simplicity, an external timing source is added. If more transmitters are available, the time is estimated together with the position of the receiver. However, the described setup uses a GPS-stabilized rubidium standard, which outputs a one Pulse Per Second (PPS) and a 10 MHz reference signal. Both signals are necessary for delivering

accurate measurements with the SDR, as the PPS signal synchronizes the full second and the 10 MHz reference increases the phase accuracy.

B. MEASUREMENT CAMPAIGN

To verify the obtained results in a real-world scenario, we conducted a measurement campaign in February 2020 in the area of Hollenstede, Germany. The receiver was placed at a distance of 30 km from the transmitter station Zeven, Germany. The received spectrum is shown in Fig. 4. We clearly identified the modulated signal and the continuous waves. Due to regulations, we were not able to transmit optimized bit sequences. However, we see that our spectrum obtained from simulation, presented in Fig. 1, presents a good match to the measured spectrum.

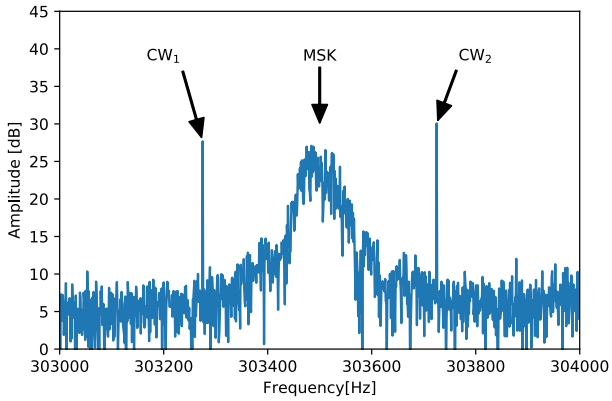

FIGURE 4. Spectra of real measurement from the station Zeven, for sample rate 1 Ms/s. CW_1, CW_2 point to the upper and lower tone, with the MSK pointing to the signal due to modulation.

Table 2 shows the variance of measured phase for an observation length of $T_{\text{obs}} = 1\text{s}$. Clearly visible, the magnitude of the variance is in the same range as for our simulation. Due to the dependence of σ^2 on the sample rate, the result does not scale with the sample rate as described earlier.

TABLE 2. Variance of the measured results in rad^2.

Sample rate	φ_1	φ_2	φ_{beat}	$\varphi_1 + \varphi_2$
1MS/s	$4.59 \cdot 10^{-5}$	$4.4 \cdot 10^{-5}$	$5.23 \cdot 10^{-5}$	$8.99 \cdot 10^{-5}$
5MS/s	$3.86 \cdot 10^{-5}$	$3.89 \cdot 10^{-5}$	$4.57 \cdot 10^{-5}$	$7.75 \cdot 10^{-5}$

As expected from section III, the estimation of each continuous wave is not statistically independent anymore, as we see in the columns φ_{beat} and $\varphi_1 + \varphi_2$. It is important to notice that we have a common clock error on our estimations, which leads to reduced performance on the estimation of φ_1 and φ_2

VI. CONCLUSION

The paper presented three signal models for the MF R-Mode and show the Cramér-Rao lower bound to estimate the phase offset for a single and the beat wave for each model. At the beginning, a simple additive model of two sinusoids was described, which showed that the lower bound depends on the variance of noise, amplitude of the tone and number of samples observed. The bound was obtained under the assumption that each tone has an integer number in Hertz as a frequency and an observation time of full seconds. We observed that for the beat frequency, the lower bound equals the sum of variance for two tones, therefore in the optimum case, the single-tone estimates are statistically independent.

The second model extends the additive signal with the addition of an MSK modulated one. We observe that in general, the estimates for the beat phase are no longer independent. However, we have found bit patterns that approach the optimal performance, which equals the bound of the model before.

When we extended the first model with a changing phase due to the velocity of the receiver, we observed a more complex bound, whose detailed presentation is beyond the scope of this paper. However, when we assume that we know the frequency shift, which is also an integer value, we derive the same bounds as before. It is therefore possible to improve the estimates through a sensor fusion approach, as the velocity is a state in PNT systems [3].

Overall, we could generalize the lower bound for the single and beat tone in (48), and show that the variance scales inversely to observation time and bandwidth of the estimator. We verified our theoretical results with simulations, which give us a good match. Moreover, we conducted real measurements, which are comparable to the presented simulation.

In general, the Cramér-Rao bound of a single tone is valid within the system. However, due to the modulation, this bound will never be reached in reality. For long observation times, the influence becomes smaller, but in order to obtain the results in near real time, they were limited in observation length. Therefore the effect cannot be neglected. However, we presented an optimized bit pattern that lowered this influence. In the future, the bound of the beat phase can be used to improve the existing coverage predictions, with respect to the range ambiguity [13]. Moreover, as we found a generalized lower bound including MSK, it can be used to improve the future realization of the estimator and to mitigate the influence of the modulation. The optimized bit pattern can also be used to design an optimized navigation message, where we design the waveform to mitigate the correlation between the MSK modulated signal and the CWs.

REFERENCES

[1] M. G. Amin, P. Closas, A. Broumandan, and J. L. Volakis, "Vulnerabilities, threats, and authentication in satellite-based navigation systems [scanning the issue]," *Proc. IEEE*, vol. 104, no. 6, pp. 1169–1173, Jun. 2016.

[2] A. Jafarnia-Jahromi, A. Broumandan, J. Nielsen, and G. Lachapelle, "GPS vulnerability to spoofing threats and a review of antispoofing techniques," *Int. J. Navigat. Observ.*, vol. 2012, Jul. 2012, Art. no. 127072.

[3] R. Ziebold, D. Medina, M. Romanovas, C. Lass, and S. Gewies, "Performance characterization of GNSS/IMU/DVL integration under real maritime jamming conditions," *Sensors*, vol. 18, no. 9, pp. 1–20, 2018.

[4] D. Medina, C. Lass, E. P. Marcos, R. Ziebold, P. Closas, and J. Garcia, "On GNSS jamming threat from the maritime navigation perspective," in *Proc. 22nd Int. Conf. Inf. Fusion (FUSION)*, 2019, pp. 1–7.
[5] E. P. Marcos, S. Caizzone, A. Konovaltsev, M. Cuntz, W. Elmarissi, K. Yinusa, and M. Meurer, "Interference awareness and characterization for GNSS maritime applications," in *Proc. IEEE/ION Position, Location Navigat. Symp. (PLANS)*, Apr. 2018, pp. 908–919.
[6] G. Johnson, P. Swaszek, J. Alberding, M. Hoppe, and J.-H. Oltmann, "The feasibility of R-mode to meet resilient PNT requirements for E-navigation," in *Proc. ION-GNSS*, 2014, pp. 3076–3100.
[7] Q. Hu, Y. Jiang, J. Zhang, X. Sun, and S. Zhang, "Development of an automatic identification system autonomous positioning system," *Sensors*, vol. 15, no. 11, pp. 28574–28591, Nov. 2015.
[8] M. Wirsing, A. Dammann, and R. Raulefs, "Designing a ranging signal for use with VDE R-mode," in *Proc. IEEE/ION Position, Location Navigat. Symp. (PLANS)*, Apr. 2020, pp. 822–826.
[9] F. Lázaro, R. Raulefs, W. Wang, F. Clazzer, and S. Plass, "VHF data exchange system (VDES): An enabling technology for maritime communications," *CEAS Space J.*, vol. 11, no. 1, pp. 55–63, Mar. 2019.
[10] G. Johnson and P. Swaszek, "Feasibility study of R-mode using AIS transmissions," Alion Sci. Technol., Tech. Rep., 2014.
[11] *Technical Characteristics of Differential Transmissions Forglobal Navigation Satellite Systems From Maritimeradio Beacons in the Frequency Band 283.5-315 kHz in Region 1 and 285-325 kHz in Regions 2 and 3*, document Recommendation ITU-R M.823-2, ITU-R, 1997.
[12] IALA Information. (2020). *Table of DGNSS Stations Edition 1.3*. [Online]. Available: https://www.iala-aism.org/content/uploads/2020/03/Table-of-DGNSS-stations-Jan-2020-final-v1.3.pdf
[13] P. Koch and S. Gewies, "Worldwide availability of maritime medium-frequency radio infrastructure for R-mode-supported navigation," *J. Mar. Sci. Eng.*, vol. 8, no. 3, p. 209, Mar. 2020, doi: 10.3390/jmse8030209.
[14] G. Johnson and P. Swaszek, "Feasibility study of R-mode using MF DGPS transmissions," Alion Sci. Technol., Tech. Rep., 2014.
[15] D. Medina, J. Vilà-Valls, E. Chaumette, F. Vincent, and P. Closas, "Cramér-Rao bound for a mixture of real- and integer-valued parameter vectors and its application to the linear regression model," *Signal Process.*, vol. 179, Feb. 2020, Art. no. 107792.
[16] D. Rife and R. Boorstyn, "Single tone parameter estimation from discrete-time observations," *IEEE Trans. Inf. Theory*, vol. IT-20, no. 5, pp. 591–598, Sep. 1974.
[17] M. Hoppe, A. Grant, C. Hargreaves, and P. Williams, "R-mode: The story so far," in *Proc. IALA Conf.*, 2018.
[18] D. C. Rife and R. R. Boorstyn, "Multiple tone parameter estimation from discrete-time observations," *Bell Syst. Tech. J.*, vol. 55, no. 9, pp. 1389–1410, Nov. 1976.
[19] S. M. Kay, *Fundamentals of Statistical Signal Processing: Estimation Theory*. Upper Saddle River, NJ, USA: Prentice-Hall, 1993.
[20] S. Pasupathy, "Minimum shift keying: A spectrally efficient modulation," *IEEE Commun. Mag.*, vol. 17, no. 4, pp. 14–22, Jul. 1979.
[21] L. Grundhöfer and S. Gewies, "R-mode receiver development for medium frequency signals," *Sci. J. Maritime Univ. Szczecin*, no. 56, pp. 57–62, 2018.
[22] S. Schuster, S. Scheiblhofer, and A. Stelzer, "The influence of windowing on bias and variance of DFT-based frequency and phase estimation," *IEEE Trans. Instrum. Meas.*, vol. 58, no. 6, pp. 1975–1990, Jun. 2009.

LARS GRUNDHÖFER (Graduate Student Member, IEEE) received the B.S. and M.S. degrees in electrical engineering from the Hamburg University of Technology, Hamburg, Germany, in 2015 and 2017, respectively.

He is currently a Scientist working for the German Aerospace Center, Institute of Communications and Navigation. His research interest includes terrestrial maritime navigation in the medium frequency band.

STEFAN GEWIES received the Diploma degree in physics from the University of Heidelberg, in 2003. He graduated from the University of Heidelberg, in 2009, with a focus on the topic of modelling solid oxide fuel cells with Ni/YSZ cermet anodes.

He joined the German Aerospace Center, Institute of Communications and Navigation, in 2009, where he started working on GNSS applications and further development of the GNSS experimentation and verification network EVnet. Since 2015, he has been led the working group Maritime Services of the department Nautical Systems. His research interest includes maritime terrestrial navigation systems.

GIOVANNI DEL GALDO (Member, IEEE) received the degree in telecommunications engineering from Politecnico di Milano, and the Ph.D. degree from Technische Universität Ilmenau, in 2007, with a focus on the topic of MIMO channel modeling for mobile communications.

He joined the Fraunhofer Institute for Integrated Circuits IIS, where he working on audio watermarking and parametric representations of spatial sound. Since 2012, he has been led a joint research group composed of a department with the Fraunhofer IIS. He was a Full Professor and the Chair with TU Ilmenau, where he focuses on the research area of wireless distribution systems and digital broadcasting. Since 2016, the group has merged with the Chair Electronic Measurements led by Prof. Reiner Thomä, giving birth to the Electronic Measurements and Signal Processing (EMS) Group. Since 2017, he has been the Director of the Institute for Information Technology, TU Ilmenau, and he leads the VDE-ITG Expert Group HF.2 on Radio Systems. His research interests include the analysis, modeling, and manipulation of multi-dimensional signals, over-the-air testing for terrestrial and satellite communication systems, and sparsity promoting reconstruction methods.